

Low-frequency $1/f$ noise in doped manganite grain-boundary junctions

J. B. Philipp, L. Alff, A. Marx,* and R. Gross

Walther-Meissner-Institut, Bayerische Akademie der Wissenschaften, Walter-Meissner-Straße 8, D-85748 Garching, Germany

(Received 28 August 2002; published 20 December 2002)

We have performed a systematic analysis of the low-frequency $1/f$ noise in single grain-boundary junctions in the colossal magnetoresistance material $\text{La}_{2/3}\text{Ca}_{1/3}\text{MnO}_{3-\delta}$. The grain-boundary junctions were formed in epitaxial $\text{La}_{2/3}\text{Ca}_{1/3}\text{MnO}_{3-\delta}$ films deposited on SrTiO_3 bicrystal substrates, and show a large tunneling magnetoresistance of up to 300% at 4.2 K as well as ideal, rectangular shaped resistance versus applied magnetic field curves. Below the Curie temperature T_C the measured $1/f$ noise is dominated by the grain boundary. The dependence of the noise on bias current, temperature, and applied magnetic field gives clear evidence that the large amount of low-frequency noise is caused by localized sites with fluctuating magnetic moments in a heavily disordered grain boundary region. At 4.2 K additional temporally unstable Lorentzian components show up in the noise spectra that are most likely caused by fluctuating clusters of interacting magnetic moments. Noise due to fluctuating domains in the junction electrodes is found to play no significant role.

DOI: 10.1103/PhysRevB.66.224417

PACS number(s): 75.30.Vn, 73.50.Td, 72.70.+m

I. INTRODUCTION

Doped manganites have attained large interest in recent years because of the interesting interplay of charge, spin, orbital, and structural degrees of freedom in these materials,¹ and their potential use in magnetoresistive devices. It was found early that the introduction of artificial grain boundaries (GB's) into epitaxial manganite thin films leads to localized structural distortions at the GB's entailing significant modifications of the magnetotransport properties of the GB's.²⁻¹⁰ In particular, a significant increase of the low-field magnetoresistance was found. Recently, in well-defined, individual GB junctions fabricated by depositing epitaxial manganite films on SrTiO_3 bicrystal substrates, a large two-level magnetoresistance effect with a maximum tunneling magnetoresistance (TMR) of up to 300% at 4.2 K has been demonstrated at low applied fields of about 200 Oe.^{9,11} These artificial GB junctions showed an almost ideal two-level resistance switching behavior with sharp transitions from low to high resistance states when the magnetic field was applied within the film plane parallel to the GB barrier. Thus manganite GB junctions represent ferromagnetic (FM) tunnel junctions with very high TMR values and a very simple fabrication process. On the other hand, the charge transport mechanism across the GB barrier has not yet been unambiguously clarified. In well-defined bicrystal GB junctions defined by growing epitaxial manganite films on SrTiO_3 bicrystal substrates, the GB barrier is formed by a straight distorted GB interface with a width of only a few nm, as shown by transmission electron microscopy.^{8,12,13} After annealing in oxygen atmosphere, individual GB junctions with large TMR values have been achieved.^{5,6,8,9,11}

Up to now, several theoretical models have been proposed^{7-10,14-16} to describe the magnetotransport properties of manganite GB junctions. However, the proposed models are controversial, and a thorough understanding of the magnetotransport properties of the GB junctions is still lacking what is mainly related to the unknown structural and magnetic properties of the GB barrier. Whereas Hwang *et al.*,³ proposed a model based on spin-polarized tunneling between ferromagnetic grains through an insulating GB bar-

rier, Evetts *et al.*¹⁴ proposed the polarization of the GB region by adjacent magnetically soft grains. Later on, Guinea¹⁶ pointed out that tunneling via paramagnetic impurity states in the GB barrier probably plays an important role, and Ziese¹⁰ suggested a description of the transport characteristics of GB's based on tunneling via magnetically ordered states in the barrier. Our recent systematic study of the magnetotransport properties of well-defined individual bicrystal GB junctions suggested a multistep inelastic tunneling process via magnetic impurity states within a disordered GB barrier.^{7-9,17} Within this model both the nonlinear current-voltage characteristics and the strong temperature and voltage dependence of the tunneling magnetoresistance could be naturally explained. In our model, strain and structural distortions at the GB interface result in a localization of charge carriers, and thereby a suppression of the ferromagnetic double exchange resulting in an insulating GB barrier with a large density of magnetic impurity states. We also pointed out that band bending effects may play an important role, resulting in a depletion layer at the GB interface below the Curie temperature of the ferromagnetic grain.⁸

Here we report on a systematic analysis of the low-frequency $1/f$ noise of individual $\text{La}_{2/3}\text{Ca}_{1/3}\text{MnO}_{3-\delta}$ bicrystal GB junctions to further clarify the transport mechanism across the GB interface. The investigation of the low-frequency $1/f$ noise properties has already proven to be a valuable tool to provide more insight into transport mechanisms across grain boundaries in the structurally related cuprate superconductors.¹⁸⁻²⁰ Therefore, a detailed evaluation of the $1/f$ noise of manganite GB junctions is highly desirable from both basic physics and application points of view.

For epitaxial thin films of doped manganites there have been several reports on a large low frequency $1/f$ noise.²¹⁻²⁵ In particular, a large noise peak close to the Curie temperature T_C has been interpreted in terms of a percolative nature of the transition between charge-ordered insulating and ferromagnetic metallic states.^{26,27} Reutler *et al.*²⁸ showed that the unusually large noise level is not an intrinsic property of the doped manganites. They found a strong coupling between local magnetic disorder and structural disorder intro-

duced by strain effects due to a lattice mismatch between film and substrate. In particular the large $1/f$ noise level was found to be absent in high-quality, strain-free epitaxial films except for a narrow peak close to T_C which is already suppressed by very small magnetic fields and is most probably due to the magnetic-phase transition, as discussed in Ref. 28. Palanisami *et al.*²⁹ suggested two different mechanisms for the noise in manganite films: fluctuations between metallic and insulating phases on the one hand, and magnetic orientation fluctuations (domain wall effects) on the other hand. Non-Gaussian properties of the noise together with random telegraph signals were taken as an experimental hint to phase segregation in colossal magnetoresistance (CMR) materials.^{30,31} On the other hand, random telegraph signals observed close to T_C were taken as evidence for a domain-wall-motion picture of the kinetics of the responsible two-level system.³²

In contrast to epitaxial thin films there are almost no experimental data on the noise properties of grain boundaries in the doped manganites. Recently, Mathieu *et al.* investigated the zero-field low-frequency noise in GB junctions in $\text{La}_{2/3}\text{Sr}_{1/3}\text{MnO}_{3-\delta}$ (Ref. 33) below the ferromagnetic transition temperature, as well as the magnetic-field dependence of the noise. They concluded that the low-field noise was due to the multidomain structure neighboring the GB, i.e., of magnetic origin. Additional Lorentzian contributions were attributed to thermally activated domain wall motion in the domain configuration close to the GB.

In this paper we present a systematic study of the low-frequency $1/f$ noise in individual grain-boundary junctions formed in $\text{La}_{0.67}\text{Ca}_{0.33}\text{MnO}_3$ films. In particular, we discuss the dependence of the measured noise on bias current, temperature, and applied magnetic field. Our results show that below T_C the noise is dominated by the GB and not by the adjacent grains. The analysis of the noise characteristics shows that the GB noise is due to localized states with fluctuating magnetic moments in a strongly disordered GB barrier. At the lowest temperatures (≈ 4.2 K) additional Lorentzian contributions show up in the noise spectra. These Lorentzians are most likely due to an ensemble of interacting magnetic impurity states giving rise to a simultaneous switching of their magnetic moments.

II. SAMPLE PREPARATION AND EXPERIMENTAL TECHNIQUES

To achieve well-defined individual manganite grain boundary junctions (GBJ's) first about 80 nm thick $\text{La}_{2/3}\text{Ca}_{1/3}\text{MnO}_{3-\delta}$ films were grown by pulsed laser deposition on symmetrical [001] tilt SrTiO_3 bicrystal substrates with a misorientation angle of 24° . For details of the preparation process, see Ref. 12. The $\text{La}_{2/3}\text{Ca}_{1/3}\text{MnO}_{3-\delta}$ films typically had a Curie temperature $T_C = 210$ K. After film deposition the films were annealed *ex situ* at 950°C in pure oxygen atmosphere. Then, typically $30\text{-}\mu\text{m}$ -wide microbridges straddling the grain boundary as well as the current and voltage leads are patterned into the biepitaxial $\text{La}_{2/3}\text{Ca}_{1/3}\text{MnO}_{3-\delta}$ films using optical lithography and Ar-ion beam etching. For comparison, microbridges of the same

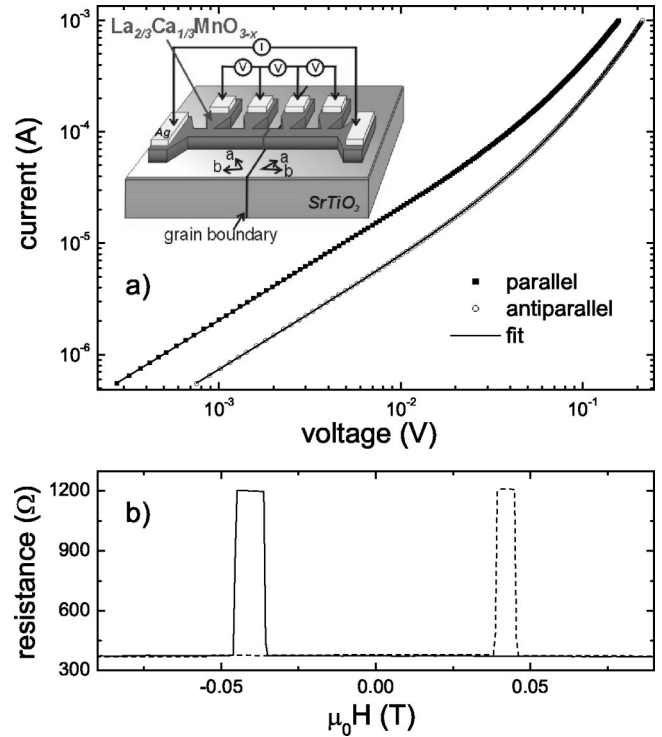


FIG. 1. (a) Current-voltage characteristics of a 24° [001] tilt GBJ in a 80-nm-thick $\text{La}_{2/3}\text{Ca}_{1/3}\text{MnO}_{3-\delta}$ film for parallel and antiparallel magnetization direction in the electrodes at $T = 40$ K. The voltage drop across the adjacent film parts has been subtracted. The solid lines are fits to the Glazman-Matveev model. The inset shows a sketch of the sample configuration. (b) Resistance vs applied magnetic-field curve at $T = 4.2$ K showing the almost ideal switching behavior of the junction resistance. The field was applied within the film plane parallel to the grain boundary.

spatial dimension that are not positioned across the grain boundary were patterned into the epitaxial film. A sketch of the sample geometry is shown in the inset of Fig. 1(a). The GBJ's fabricated in this way were characterized by measuring the current-voltage characteristics as functions of temperature and applied magnetic field. After the annealing process the GBJ's show an almost perfect two-level resistance switching behavior with sharp transitions between the low and high resistance levels as already reported recently.¹¹

The noise properties of the GBJ's were measured by biasing the junctions at a constant current I_b and measuring the low-frequency voltage fluctuations superimposed on the resulting junction voltage. The voltage fluctuations were amplified by low-noise amplifiers and subsequently processed by a digital spectrum analyzer. In this way noise spectra have been taken in the frequency range from 1 Hz to 100 kHz. The measurements were performed as a function of temperature (4.2–300 K) and applied magnetic field (up to 12 T). The magnetic field always was applied within the film plane parallel to the GB barrier. Great care has been taken of the electromagnetic shielding of the sample during the noise measurements.

In the following we will quantify the measured voltage noise power by the frequency independent normalized voltage noise power:

$$\Gamma = \frac{S_V}{V^2} \times f^\alpha. \quad (1)$$

Here S_V is the spectral density of the voltage fluctuations and the exponent α usually is close to unity. Below, we will usually plot the octave integral

$$P_{\text{octave}} = \int_{f_1}^{2f_1} \frac{S_V}{V^2} df. \quad (2)$$

For $S_V \propto 1/f$ we have $P_{\text{octave}} = \Gamma \ln 2$.

III. EXPERIMENTAL RESULTS AND DISCUSSION

A. Transport and noise data

We first discuss the electrical transport properties of the GBJ's. Typical current-voltage characteristics (IVC's) of a $\text{La}_{2/3}\text{Ca}_{1/3}\text{MnO}_{3-\delta}$ GBJ are shown in Fig. 1(a). For the parallel magnetization direction in the electrodes the highly nonlinear IVC's can be accurately described within the Glazman-Matveev (GM) model³⁴ for all temperatures below T_C . Within the GM model the transport of charge carriers across a barrier containing a significant number of defect states is mediated both by elastic tunneling (direct or resonant tunneling via a single impurity state) and by inelastic tunneling processes via two and more defect states. Within this model the IVC's can be expressed by

$$I = G_1 V + G_2 V^{7/3} + G_3 V^{7/2} + \dots, \quad (3)$$

where G_1 is the elastic contribution of direct and resonant tunneling via a single localized state and G_2, G_3, \dots give the inelastic contribution to the total current from tunneling involving 2, 3, . . . impurity states. The solid lines in Fig. 1(a) represent fits of Eq. (3) to the experimental data taking into account tunneling channels up to $n=3$ localized states.⁹ Channels with $n>3$ are found to give only negligible contributions. For the antiparallel magnetization configuration the GM model also describes the IVC's at $T \approx 40$ K well. We note, however, that for other temperatures the agreement with the GM prediction for the antiparallel configuration was not as perfect as shown in Fig. 1(a).

In Fig. 1(b) we show the resistance versus applied magnetic field curve for the magnetic field applied within the film plane parallel to the grain boundary. As discussed in detail elsewhere,¹¹ for this field direction the grain boundary junctions show an almost ideal rectangular-shaped switching behavior between the low resistance state with a parallel magnetization orientation and the high resistance state with an antiparallel magnetization orientation in the junction electrodes.

We next discuss the noise data. Figure 2 shows the temperature dependence of the normalized octave noise power P_{octave} for two $\text{La}_{2/3}\text{Ca}_{1/3}\text{MnO}_{3-\delta}$ microbridges of similar geometry. Whereas one microbridge is straddling the GB, i.e., contains an individual GBJ, the other is not positioned across the GB, i.e., does not contain a GBJ. By comparing the noise data of these two microbridges we can clearly identify the contribution of the GBJ to the measured noise. The

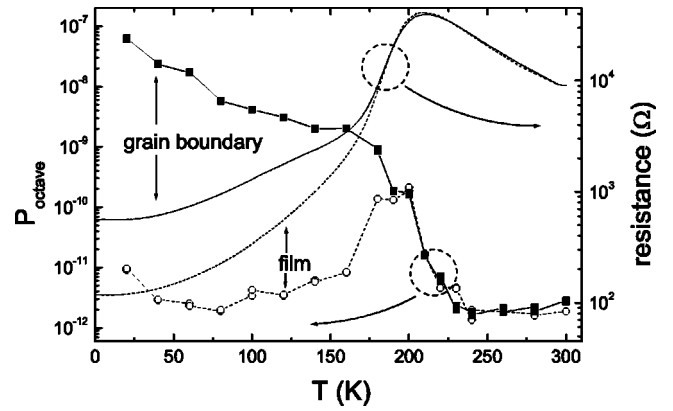


FIG. 2. Temperature dependence of the normalized noise power plotted as octave integral from 100 to 200 Hz for a microbridge with (full symbols, solid line) and without a GB (open symbols, dashed line). The noise spectra have been taken at a sample voltage of $V = 100$ mV. For comparison the temperature dependence of the resistance is also shown.

$1/f$ noise for the microbridge with the GBJ is rapidly increasing with decreasing temperature for $T < 220$ K. In contrast, the noise of the microbridge without GBJ is almost temperature independent except for a peak close to T_C . We recently showed that this noise peak can be suppressed by a small applied magnetic field and is related most likely to magnetic fluctuations at the paramagnetic to ferromagnetic transition in the doped manganites.²⁸ The key result of Fig. 2 is the fact that below T_C the $1/f$ noise power of the microbridge with a GBJ is orders of magnitude larger than the noise power of the epitaxial film. That is, for the microbridge with a GBJ the measured noise can be attributed to the GBJ alone, since the additional noise of the adjacent grains is negligibly small.

Although we do not want to discuss the details of the noise of the epitaxial $\text{La}_{2/3}\text{Ca}_{1/3}\text{MnO}_{3-\delta}$ film, we briefly compare the noise data of the epitaxial film shown in Fig. 2 to those reported in our previous study.²⁸ In Ref. 28 we have analyzed the low-frequency noise in highly strained $\text{La}_{2/3}\text{Ca}_{1/3}\text{MnO}_{3-\delta}$ films grown on SrTiO_3 substrates. The magnitude of the noise measured for these strained films is much larger than that measured for the $\text{La}_{2/3}\text{Ca}_{1/3}\text{MnO}_{3-\delta}$ films of our present study, although the $\text{La}_{2/3}\text{Ca}_{1/3}\text{MnO}_{3-\delta}$ films were grown on the same substrate (SrTiO_3) with the same lattice mismatch. These different characteristics originate in the post-deposition annealing process applied to the films of the present study. This annealing process results in a significant release of the epitaxial strain and, in turn, in a reduction of the noise amplitude. This is in agreement with our recent study, where we have shown that the noise amplitude in strained $\text{La}_{2/3}\text{Ca}_{1/3}\text{MnO}_{3-\delta}$ films is larger by many orders of magnitude than in almost strain-free films grown on NdGaO_3 substrates.²⁸ The effect of a post-deposition thermal process on the noise properties of strained manganite films was also discussed in Ref. 25.

Figure 3 shows the dependence of normalized octave noise power P_{octave} on a magnetic field applied within the film plane parallel to the GB for different values of the bias current I_b . Figure 3 shows two experimental facts. First, the

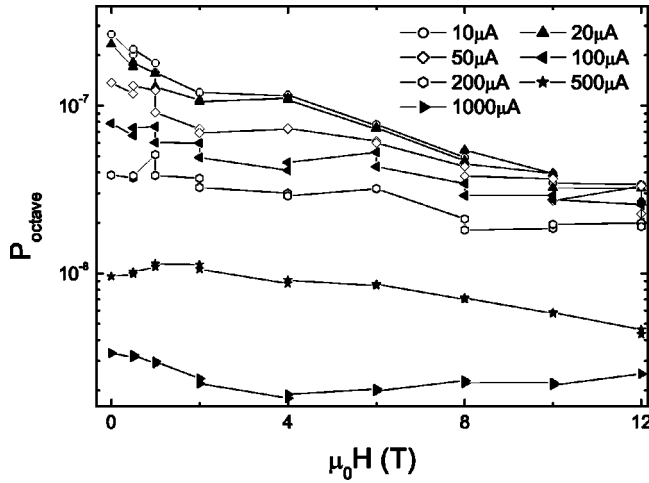


FIG. 3. Magnetic field dependence of the normalized noise power for a $\text{La}_{2/3}\text{Ca}_{1/3}\text{MnO}_{3-\delta}$ GBJ in the octave from 100 to 200 Hz at $T=40$ K for different values of the bias current I_b .

noise power decreases with increasing bias current for all applied fields for $I_b \geq 10 \mu\text{A}$. Second, the noise power decreases with increasing magnetic field for bias current values below $500 \mu\text{A}$. Whereas for $I_b \leq 100 \mu\text{A}$ the noise decreases by more than one order of magnitude by increasing the magnetic field to 12 T, for $I_b \geq 100 \mu\text{A}$ the noise is only weakly dependent on the applied magnetic field.

Figure 4 shows the detailed dependence of the normalized noise power P_{octave} on the bias current I_b for both the parallel and antiparallel magnetization direction in the GBJ electrodes at $T=40$ K. It is evident that both for the parallel and antiparallel magnetization orientations there is only a very weak bias current dependence of the normalized noise power for small bias currents followed by a rapid decrease of P_{octave} at large bias current values. As illustrated in the inset of Fig. 4, the noise power $f \times S_V(I_b)$ shows a nonlinear dependence on the bias current.

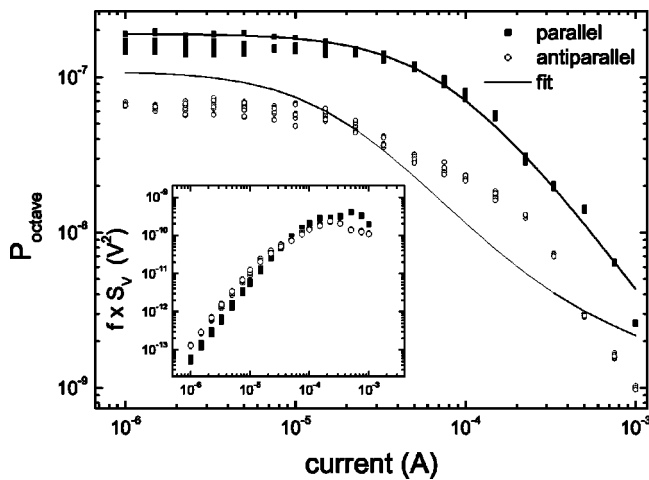


FIG. 4. Normalized noise power P_{octave} in the octave from 100 to 200 Hz plotted vs the bias current I_b for parallel (full symbols) and antiparallel magnetization direction in the GBJ electrodes (open symbols) at $T=40$ K. The solid lines are fits to the data according to the small signal analysis [cf. Eq. (5)]. The inset shows the noise power $f \times S_V$ vs the bias current I_b .

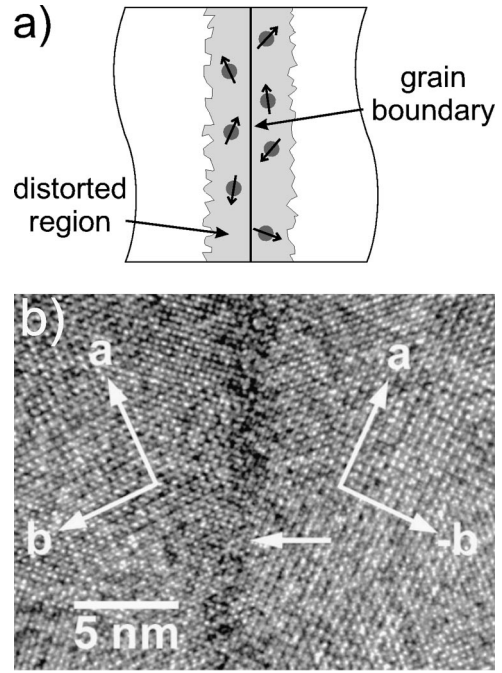


FIG. 5. (a) Sketch of the junction model for grain boundary junctions in the doped manganites. The grain boundary interface is formed by a few nm wide distorted region containing a high density of defects states carrying a magnetic moment. The transport is by elastic tunneling as well as by inelastic tunneling. (b) High-resolution transmission electron micrograph (planar view) of a grain boundary in an epitaxial $\text{La}_{2/3}\text{Ca}_{1/3}\text{MnO}_{3-\delta}$ thin film grown on a 36.8° symmetrical [001] tilt SrTiO_3 substrate. The image was obtained for a grain boundary that has not been annealed after the deposition process. The distorted grain boundary region is confined to within a few lattice spacings. The arrow marks a step along the straight grain boundary interface.

B. Model considerations

In the following we will argue that both the dc electrical transport and the low-frequency noise properties can be consistently understood in a junction model assuming a strongly distorted region at the GB containing a large number of localized states or traps with fluctuating magnetic moments. A sketch of this junction model is shown in Fig. 5(a).

It is well known from the study of GB's in other perovskite materials (e.g., cuprate superconductors^{35,36}) that strain, structural disorder, and oxygen deficiency are important factors having a strong impact on the electrical transport properties. Figure 5(b) shows a high resolution transmission electron microscopy (HR-TEM) micograph of a symmetrical 36.8° [001] tilt GB in a $\text{La}_{2/3}\text{Ca}_{1/3}\text{MnO}_{3-\delta}$ film deposited on a SrTiO_3 bicrystal substrate.¹² It is obvious that the grain-boundary region is clean without any secondary phases and that the lattice distortions are confined to within a few lattice spacings. This is very similar to GB's in the cuprate superconductors, where the boundaries were also found to be clean without any secondary phases and with the lattice distortions to be confined within 1–2 lattice spacings.^{37–39} However, the grain boundaries in doped manganite epitaxial films are almost as straight as the GB in the underlying SrTiO_3 bicrystal substrate. This is in clear contrast to GB's in

the cuprate superconductors that are strongly faceted.^{38,39} It is very likely that this difference is related to the different growth modes of the cuprate and manganite thin films. Whereas the cuprates show a pronounced island growth with the islands growing across the substrate grain boundary resulting in strong faceting, the manganites show a molecular layer-by-layer growth mode.¹² In this growth mode it is expected that the grain boundary in the film follows that of the substrate exactly. We also have preliminary results that the microstructure of GB's in the manganites significantly depends on the deposition technique (e.g. laser molecular-beam epitaxy, sputtering), the lattice mismatch between the film and the substrate and post-deposition annealing processes. However, more HR-TEM work is required for a detailed clarification of this issue.

For the cuprate GB's either a description in terms of a space-wise metal insulator transition at the grain boundary or in terms of band bending effects^{40,41} lead to a description of the GB as composed of an insulating layer at the barrier region which due to strain and structural disorder most likely contains a high density of localized defect states. Because of the structural affinity of the cuprate superconductors and the doped manganites, it is very likely that for these ferromagnetic junctions the transport properties are also determined by an insulating tunnel barrier containing a large density of localized states.⁸ Furthermore, there is already strong evidence of the presence of a significant density of localized states in the barrier from the fact that the current-voltage characteristics of the manganite GBJ's can be very well described within the GM model (cf Fig. 1). Further evidence comes from the strong temperature and voltage dependence of the low-field tunneling magnetoresistance.⁹ Based on this experimental evidence we recently proposed that the magnetotransport in manganite GBJ's is determined by multistep inelastic tunneling via magnetic impurity states within a disordered insulating GB barrier.⁷⁻⁹

Based on the model assumption of a large number of localized states within an insulating GB barrier there are two possible mechanisms which may be responsible for the observed low frequency voltage fluctuations. First, the localized defect states are capable of trapping and releasing charge carriers. This charge-carrier trapping and release processes lead to local variations of the barrier height and, thus, to fluctuations of the tunneling conductance. Furthermore, the magnetic field dependence of the noise (cf. below) suggests that the charge traps are associated with a magnetic moment with a fluctuating orientation. Then both the trapping and release of the charge carriers and, hence, the charge transport between the highly spin-polarized electrodes depend on the local magnetic moment of the charge traps. Since the trapping and releases process depends on the relative orientation of the magnetic moment of the trap and the electrode magnetization, fluctuations of the direction of the magnetic moments of the charge traps strongly influence the local barrier transparency. A second mechanism giving rise to low-frequency noise is related to coupling between the localized magnetic moments \mathbf{S}_L of the localized states and the spin \mathbf{s} of the tunneling electrons. Within the simplest approximation this coupling gives rise to an additional po-

tential energy $U(\alpha) = J\mathbf{S}_L \cdot \mathbf{s} = JS_L s \cos \alpha$, where J is the coupling constant and α the angle between the localized moment and the electron spin. This additional energy, which is fluctuating with fluctuating orientation of the localized magnetic moments, can be viewed as a fluctuation of the local barrier height.

Within the model of local barrier height fluctuations the dependence of the normalized voltage noise power P_{octave} on the bias current can be described within a small signal analysis based on the GM model. Doing so, we assume that the voltage fluctuations are caused by fluctuations of both the elastic and inelastic current contributions due to temporal variations of the local barrier height. Considering fluctuations of the elastic G_1 and inelastic G_2 and G_3 term, Eq. (3) gives, for the small signal voltage fluctuation,

$$\begin{aligned} \delta V &\approx \frac{\partial V}{\partial G_1} \delta G_1 + \frac{\partial V}{\partial G_2} \delta G_2 + \frac{\partial V}{\partial G_3} \delta G_3 + \dots \\ &\approx V \frac{\delta G_1}{\tilde{G}} + V^{7/3} \frac{\delta G_2}{\tilde{G}} + V^{7/2} \frac{\delta G_3}{\tilde{G}}, \end{aligned} \quad (4)$$

where $\tilde{G} = [G_1 + \frac{7}{3}G_2V^{4/3} + \frac{7}{2}G_3V^{5/2}]$ roughly corresponds to the total tunneling conductance. For independent fluctuations δG_1 , δG_2 , and δG_3 , the normalized voltage noise

$$\frac{S_V}{V^2} = \frac{S_{G_1}}{\tilde{G}^2} + V^{8/3} \frac{S_{G_2}}{\tilde{G}^2} + V^5 \frac{S_{G_3}}{\tilde{G}^2} \quad (5)$$

is determined by the normalized fluctuations $S_{G_1}/\tilde{G}^2 = (\delta G_1/\tilde{G})^2$, $S_{G_2}/\tilde{G}^2 = (\delta G_2/\tilde{G})^2$, and $S_{G_3}/\tilde{G}^2 = (\delta G_3/\tilde{G})^2$ of the GM coefficients.

Analyzing Eqs. (4) and (5) we can conclude the following: At low bias current (junction voltage) the elastic tunneling current is dominating and we can neglect the S_{G_2} and S_{G_3} terms, and furthermore can use the approximation $\tilde{G} \approx G_1$. Hence for a low bias current we expect $S_V/V^2 \approx S_{G_1}/G_1^2$, that is, a normalized noise power independent of the bias current (junction voltage). With increasing bias current (junction voltage) the inelastic tunneling contribution no longer can be neglected. This results in an increase of \tilde{G} with increasing voltage and, hence, in an overall decrease of $S_V/V^2 \propto 1/\tilde{G}^2$, even if the noise contributions of the inelastic channels increase with increasing voltage. As shown in Fig. 4 this behavior expected from our model consideration is in good qualitative agreement with the measured data.

We even can go further and fit the data by Eq. (5). The solid lines in Fig. 4 are fits of Eq. (5) to the experimental data, taking into account only fluctuations of the elastic G_1 term and the first inelastic G_2 term. That is, S_{G_1} and S_{G_2} have been used as fit parameters, and the term S_{G_3} has been neglected to keep the number of fitting parameters minimum. We note that the GM coefficients G_1 , G_2 , and G_3 entering \tilde{G} are obtained by fitting the current-voltage characteristics by the GM model prediction, and therefore are fixed param-

eters in the fit of the noise data. Figure 4 shows that the small signal noise analysis based on the GM model is in good agreement with the experimental data for parallel magnetization alignment in the junction electrodes. The values for the normalized fluctuations in the elastic channel $S_{G_1}/G_1^2 \approx 10^{-7}$ obtained from the numerical fits can be compared to the noise data of GBJ's in cuprate superconductors, since $(\delta G/G)^2 = (\delta R/R)^2$, where $\delta R/R$ are the normalized junction resistance fluctuations.⁴² The normalized G_1 fluctuations nicely follow the scaling discussed in Ref. 42 for the cuprate superconductors. This scaling behavior has been discussed in terms of a constant density of trapping centers in the cuprate GBJ's. Therefore, the noise data of the manganite GBJ's give further evidence of the close similarity to cuprate GBJs and suggest a similar density of the noise centers in both junction types. Furthermore, S_{G_1} and S_{G_2} are found to depend only weakly on temperature in the investigated temperature range below 80 K.

For the antiparallel magnetization orientation in the junction electrodes the modeling of the noise data by a small signal noise analysis based on the GM model is less convincing. However, Fig. 4 shows that a similar overall dependence of the normalized noise power on the bias current is observed for the antiparallel magnetization orientation. This is expected if we suppose that we can use the simple Jullière model⁴³ to describe the ferromagnetic tunnel junction. Within this model the tunneling current is given by the tunneling matrix element and the density of states $N_{\uparrow\downarrow}(E_F)$ of the two spin directions at the Fermi level in the junction electrodes. Going from the parallel to the antiparallel configuration the tunneling matrix element stays the same. However, for a material with finite spin polarization the density of states $N_{\uparrow\downarrow}(E_F)$ for the spin-up and spin-down electrons is changed. Since in the elastic tunneling process the spin direction is conserved, a reduction of G_1 and S_{G_1} is expected going from the parallel to the antiparallel magnetization orientation. It was shown recently⁹ that in the inelastic tunneling processes the spin direction does not seem to be conserved in manganite GBJ's. Therefore, no reduction of G_2 and G_3 as well as S_{G_2} is expected going from the parallel to the antiparallel magnetization orientation. Then, according to Eq. (5), we expect a slightly reduced value of S_V/V^2 and a similar functional dependence on the bias current (junction voltage). This is in qualitative agreement with the experimental data. We note, however, that the Jullière model certainly is too simple to describe the junction behavior in full detail. In particular, the assumption of a voltage-independent density of states for the two spin directions may be an insufficient approximation. Recently, it was shown that band structure effects give rise to voltage-dependent currents that conserve spin.⁴⁴ Summarizing our discussion we can conclude that our simple model based on an insulating tunneling barrier containing a high density of localized defect states already describes (at least for the parallel magnetization orientation) the measured noise data in a sufficient way. In order to get an even better agreement more sophisticated models have to be taken into consideration.

We now discuss the dependence of Γ or, equivalently, P_{octave} on temperature. As shown in Fig. 2, we observe an increase of P_{octave} with decreasing temperature. This is expected within our model due to the increase of the spin polarization in the junction electrodes with decreasing temperature.⁹ In this case the fluctuating orientation of the localized magnetic moments within the GB barrier results in increasing fluctuations of the local barrier height. Whereas for a random orientation of the electron spin (zero spin polarization) a change of the direction of the local magnetic moments does not change anything and hence does not influence the tunneling probability, for a full orientation of the electron spins (100% spin polarization) each orientation of the localized magnetic moments corresponds to a different potential energy $U_L = JS_L \cdot s$ and hence a different local barrier height. That is with increasing spin polarization the fluctuations of the orientation of the localized moments results in increasing fluctuations of the local barrier height. We note that judging from the evaluation of the IVC's within the GM model the average barrier transparency is almost independent of temperature.

We next discuss the dependence of P_{octave} on the applied magnetic field. Applying a magnetic field was found to continuously decrease the junction noise up to 12 T for bias currents $\leq 500 \mu\text{A}$, as shown in Fig. 3. This can be explained within the proposed model in a straightforward way. The applied magnetic field tends to align the localized magnetic moments of the charge traps in the barrier region and thus reduces the fluctuations of the potential energy $U_L = JS_L \cdot s$ and, hence, the fluctuations of the local barrier height. We note, however, that in order to explain the magnetic field dependence of the noise power up to the largest applied field of 12 T (see Fig. 3) the fluctuating magnetic moments associated with the localized states cannot be considered as free moments but rather as (weakly) interacting moments forming a spin glass like state. It is well known that the physics of the doped manganites is determined by a competition of ferromagnetic double exchange and antiferromagnetic superexchange between neighboring Mn ions, which sensitively depends on doping as well as structural disorder and bond angles. Of course, for bulk $\text{La}_{2/3}\text{Ca}_{1/3}\text{MnO}_{3-\delta}$ the ferromagnetic double exchange is dominating. However, for the structurally distorted GB region there is certainly a strongly suppressed double exchange resulting in locally ferromagnetic and antiferromagnetic exchange.⁴⁵ Because of this distorted nature of the GB it is plausible to assume that there is an arrangement of interacting magnetic moments strongly resembling a spin glass in the GB barrier.

We finally note that a spin polarized bias current of about $100 \mu\text{A}$ corresponding to a current density of about 10^3 A/cm^2 flowing across the GB may result in a nonvanishing orientation of the localized magnetic moments. That is, in this scenario the spin-polarized current is expected to have the same effect as an applied magnetic field, namely, to reduce the low-frequency noise. A reduction of the noise with increasing bias current has indeed been observed (see Fig. 4) but attributed above within the GM model to an increase of the inelastic tunneling current with increasing bias current (junction voltage). Since the functional form of the bias cur-

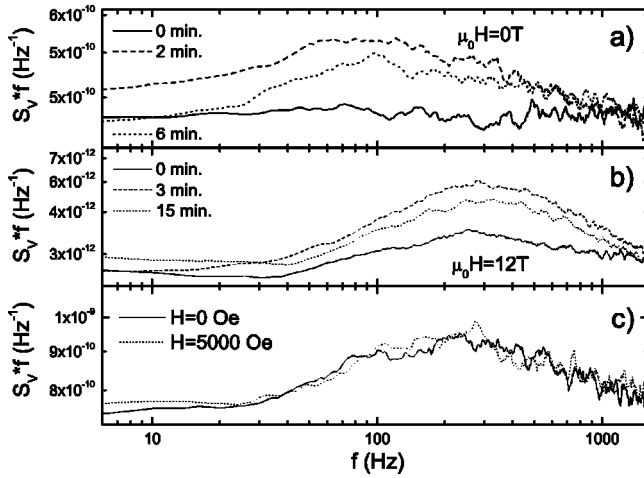


FIG. 6. Voltage noise power times frequency plotted vs frequency at 4.2 K. Additional Lorentzian noise components are present with characteristic properties: some Lorentzians evolve in time at zero magnetic field (a) as well as in an applied magnetic field up to 12 T (b). On the other hand, some Lorentzians (c) do neither change in time nor are affected by an applied magnetic field.

rent dependence of the noise fits well to the GM model based explanation, we conclude that the orientation effect of the spin polarized current, although present, is small.

At low temperature ($T=4.2$ K) we observed additional Lorentzian contributions to the low-frequency $1/f$ noise as illustrated in Fig. 6. In contrast to the experiments in Refs. 33, 46, and 47 these Lorentzians displayed various characteristic properties that are in obvious contradiction to the assumption of domain wall motion. First, we observe an evolution of the Lorentzians in time both at zero magnetic field [Fig. 6(a)] and at an applied magnetic field of $\mu_0 H=12$ T [Fig. 6(b)]. Second, as shown in Fig. 6(c) some Lorentzian components were found to be completely unaffected by applying a magnetic field as large as several hundred mT. Because of this ambiguous dependence on both time and magnetic field we suppose that the Lorentzians are due to an ensemble of interacting localized magnetic moments. The interaction between the moments leads to simultaneous switching of their direction between a discrete number of orientations. Random switching of the magnetization of such an ensemble between *two* distinct directions thus defines a two level system giving rise to random telegraph noise with a Lorentzian power spectrum. Furthermore, the independence of the Lorentzian contribution on the magnetic field shown in Fig. 6 also provides clear evidence against domain fluctuations in the junction electrodes as the origin of the GBJ noise.

To further clarify the magnetic properties of the barrier region we have investigated the magnetic field dependence of the junction resistance down to 2 K and up to 16 T. Recently, in Refs. 7 and 8 the distorted barrier was modeled as a paramagnetic (PM) region even below the Curie temperature T_C of the doped manganite, since the ferromagnetic double exchange is suppressed in the distorted GB layer. Since according to theoretical predictions⁴⁸ the paramagnetic insulator to ferromagnetic metal transition in the junction

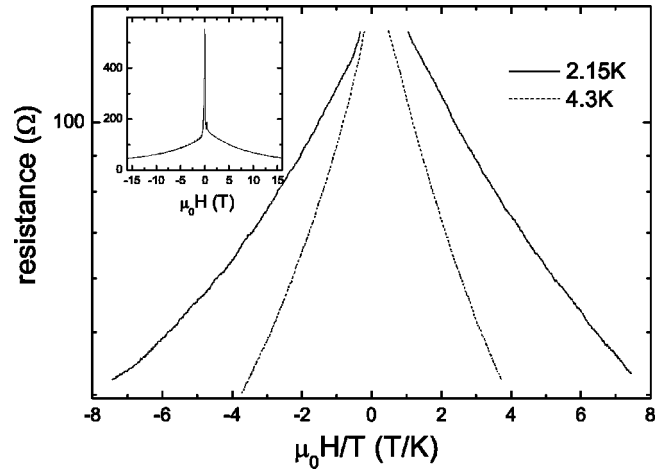


FIG. 7. Resistance of a $\text{La}_{2/3}\text{Ca}_{1/3}\text{MnO}_{3-\delta}$ GBJ plotted vs $\mu_0 H/T$ at 2.15 and 4.3 K.

electrodes is expected to result in a large shift of the chemical potential, it has been argued that considerable band bending effects occur at the GB interface below T_C . These band bending effects lead to a depletion of the paramagnetic GB layer. The width t of this depletion layer is a function of the magnetization difference $\Delta M = M_{\text{FM}} - M_{\text{PM}}$ of the FM electrodes and the PM barrier with $t \propto \Delta M$.^{7,8,48} At low temperature and fields above the coercive field the magnetization of the ferromagnetic electrodes can be assumed constant, and we have $t \propto \Delta M \propto M_{\text{PM}}$. The magnetization of the PM layer is determined by the Brillouin function, which is a function of H/T . Then, we expect $\Delta M \propto f(H/T)$ and, hence, $t \propto f(H/T)$. Then the junction resistance $R \propto \exp(-t)$ is expected to follow $R \propto \exp[-f(H/T)]$. This is clearly not observed experimentally, as shown in Fig. 7, where the two $R(H)$ curves recorded at different temperatures do not coincide when plotted versus H/T . Furthermore, for $H/T \ll 1$ the Brillouin function can be approximated by H/T . In this case $R \propto \exp(-H/T)$ is expected. Such behavior has indeed been reported,⁷ and is also shown in Fig. 7. However, for a paramagnetic GB layer at very low temperature and very high fields the $R \propto \exp(-H/T)$ behavior should no longer be valid, since the Brillouin function no longer can be approximated by H/T . In contrast, the magnetization of the paramagnetic GB barrier is expected to saturate, resulting in a saturation of the junction resistance. As shown by Fig. 7 this is clearly not observed in our experiments. Summarizing we can conclude that the absence of a H/T scaling of the measured $R(H)$ curves and of any saturation of the junction resistance at very high magnetic fields, even at 2.3 K provides further evidence that the barrier region rather resembles a spin glass than a paramagnetic material in agreement with the above conclusions drawn from the analysis of the noise data.

We also would briefly like to compare our noise data to that already available in literature. Recently, Mathieu *et al.*³³ investigated the $1/f$ noise of GB junctions in $\text{La}_{0.7}\text{Sr}_{0.3}\text{MnO}_3$ thin films. In these experiments the low-frequency noise was found to show the same dependence on an applied magnetic field as the dc resistance. Therefore, the authors suggested that the measured low-field noise is of magnetic origin re-

lated to domain fluctuations and domain wall motion in a multi-domain state neighboring the GB region. They further argued that the origin of the observed additional Lorentzian components in the low frequency noise are caused by thermally activated domain-wall motion in this domain configuration.

Our noise data do not support this picture of a fluctuating magnetic state in the junction electrodes adjacent to the GB. The accurate description of both the IVC's and the noise data within the GM model strongly supports a tunnelinglike mechanism for the charge transport and gives strong evidence that the low-frequency noise in the manganite GB junctions is caused by the trapping and release of charge carriers in localized defect states within the GB barrier. Further support for the tunnel junction model stems from the $R(H)$ dependencies.¹¹ Here, for our GBJ's, an ideal two-level resistance switching with sharp transition from the low to the high resistance state is observed with the magnetic field applied parallel to the GB barrier resembling the rectangular shaped $R(H)$ characteristics observed in TMR devices based on transition metals.⁴⁹ Such $R(H)$ dependencies would not be expected in the presence of a multidomain state in the junction electrodes. Furthermore, the normalized octave noise P_{octave} of Fig. 3 shows a strong magnetic field dependence up to applied fields of 12 T especially at low bias currents. Again, this is in contradiction to a multidomain state, for which domain fluctuations are expected to be strongly suppressed at fields above about 1 T where the domains are fully aligned.

IV. SUMMARY

In summary, we performed a detailed analysis of the low frequency $1/f$ noise in individual bicrystal grain-boundary junctions formed in epitaxial $\text{La}_{0.67}\text{Ca}_{0.33}\text{MnO}_3$ films as a function of temperature, bias current, and applied magnetic field. Our noise data show that the low-frequency noise in these junctions showing nearly ideal two-level resistance switching is due to localized sites with fluctuating magnetic moments in a strongly distorted barrier region. This is in full agreement with the description of the electrical transport properties of the GBJ's by elastic and inelastic tunneling via localized defects states within an insulating grain-boundary barrier. Low-frequency noise due to domain fluctuations in the junction electrodes is found to play no significant role in the investigated samples. Additional Lorentzian contributions to the noise showing up at low temperature are most likely caused by clusters of interacting magnetic moments. The analysis of the electrical transport properties and the noise up to high magnetic fields suggests that the grain-boundary barrier is a spin glass rather than a paramagnetic layer.

ACKNOWLEDGMENTS

The authors want to thank C. Höfener and J. Klein for valuable discussions. This work was supported by the BMBF.

*Electronic address: Achim.Marx@wmi.badw.de; URL: <http://www.wmi.badw-muenchen.de>

- ¹M. B. Salamon and M. Jaime, *Rev. Mod. Phys.* **73**, 583 (2001).
- ²M. K. Gubkin, T. M. Perekalina, A. V. Bykov, and V. A. Chubarenko, *Fiz. Tverd. Tela (St. Petersburg)* **35**, 1443 (1993) [*Phys. Solid State* **35**, 728 (1993)].
- ³H. Y. Hwang, S.-W. Cheong, N. P. Ong, and B. Barlogg, *Phys. Rev. Lett.* **77**, 2041 (1996).
- ⁴A. Gupta, G. Q. Gong, G. Xiao, P. R. Duncombe, P. Lecoeur, P. Trouilloud, Y. Y. Wang, V. P. Dravid, and J. Z. Sun, *Phys. Rev. B* **54**, R15629 (1996).
- ⁵N. D. Mathur, G. Burnell, S. P. Isaac, T. J. Jackson, B.-S. Teo, J. L. MacManus-Driscoll, L. F. Cohen, J. E. Evetts, and M. G. Blamire, *Nature (London)* **387**, 266 (1997).
- ⁶K. Steenbeck, T. Eick, K. Kirsch, K. O'Donnell, and E. Steinbeiß, *Appl. Phys. Lett.* **71**, 968 (1997).
- ⁷J. Klein, C. Höfener, S. Uhlenbruck, L. Alff, B. Büchner, and R. Gross, *Europhys. Lett.* **47**, 371 (1999).
- ⁸R. Gross, L. Alff, B. Büchner, B. H. Freitag, C. Höfner, J. Klein, Yafeng Lu, W. Mader, J. B. Philipp, M. S. R. Rao, P. Reutler, S. Ritter, S. Thienhaus, S. Uhlenbruck, and B. Wiedenhorst, *J. Magn. Magn. Mater.* **211**, 150 (2000).
- ⁹C. Höfener, J. B. Philipp, J. Klein, L. Alff, A. Marx, B. Büchner, and R. Gross, *Europhys. Lett.* **50**, 681 (2000).
- ¹⁰M. Ziese, *Phys. Rev. B* **60**, R738 (1999).
- ¹¹J. B. Philipp, C. Höfener, S. Thienhaus, J. Klein, L. Alff, and R. Gross, *Phys. Rev. B* **62**, 9248 (2000).
- ¹²R. Gross, J. Klein, B. Wiedenhorst, C. Höfener, U. Schoop, J. B.

- Philipp, M. Schonecke, F. Herbstritt, L. Alff, Yafeng Lu, A. Marx, S. Schymon, S. Thienhaus, and W. Mader, in *Superconducting and Related Oxides: Physics and Nanoengineering IV*, edited by D. Pavuna and I. Bosovic, SPIE Conf. Proc. 4058 (SPIE-Intl. Society for Optical Engineering, Bellingham, 2000), pp. 278–294.
- ¹³B. Wiedenhorst, C. Höfener, Yafeng Lu, J. Klein, M. R. S. Rao, B. H. Freitag, W. Mader, L. Alff, and R. Gross, *J. Magn. Magn. Mater.* **211**, 16 (2000).
- ¹⁴J. E. Evetts, M. G. Blamire, N. D. Mathur, S. P. Isaac, B.-S. Teo, L. F. Cohen, and J. L. MacManus-Driscoll, *Philos. Trans. R. Soc. London, Ser. A* **356**, 1593 (1998).
- ¹⁵J. M. D. Coey, A. E. Berkowitz, L. Balccells, F. F. Putris, and A. Barry, *Phys. Rev. Lett.* **80**, 3815 (1998).
- ¹⁶F. Guinea, *Phys. Rev. B* **58**, 9212 (1998).
- ¹⁷J. Zhang and R. M. White, *J. Appl. Phys.* **83**, 6512 (1998).
- ¹⁸A. Marx, U. Fath, W. Ludwig, R. Gross, and T. Amrein, *Phys. Rev. B* **51**, 6735 (1995).
- ¹⁹A. Marx, L. Alff, and R. Gross, *Appl. Supercond.* **6**, 621 (1999).
- ²⁰T. Kemen, A. Marx, L. Alff, D. Kölle, and R. Gross, *IEEE Trans. Appl. Supercond.* **9**, 3982 (1999).
- ²¹G. B. Alers, A. P. Ramirez, and S. Jin, *Appl. Phys. Lett.* **68**, 3644 (1996).
- ²²A. Lissauskas, S. I. Khartsev, and A. M. Grishin, *J. Low Temp. Phys.* **117**, 1647 (1999).
- ²³H. T. Hardner, M. B. Weissman, M. Jaime, R. E. Treece, P. C. Dorsey, J. S. Horwitz, and D. B. Chrisey, *J. Appl. Phys.* **81**, 272 (1997).

- ²⁴M. Rajeswari, A. Goyal, A. K. Raychaudhuri, M. C. Robson, G. C. Xiong, C. Kwon, R. Ramesh, R. L. Greene, T. Venkatesan, and S. Lakeou, *Appl. Phys. Lett.* **69**, 851 (1996).
- ²⁵M. Rajeswari, R. Shreekala, A. Goyal, S. E. Lofland, S. M. Bhagat, K. Ghosh, R. P. Sharma, R. L. Greene, R. Ramesh, T. Venkatesan, and T. Boettcher, *Appl. Phys. Lett.* **73**, 2672 (1998).
- ²⁶V. Podzorov, M. Uehara, M. E. Gershenson, T. Y. Koo, and S.-W. Cheong, *Phys. Rev. B* **61**, 3784 (2000).
- ²⁷A. Anane, B. Raquet, S. von Molnár, L. Pinsard-Godart, and A. Revcolevschi, *J. Appl. Phys.* **87**, 5025 (2000).
- ²⁸P. Reutler, A. Bensaid, F. Herbstritt, C. Höfener, A. Marx, and R. Gross, *Phys. Rev. B* **62**, 11619 (2000).
- ²⁹A. Palanisami, R. D. Merithew, M. B. Weissman, and J. N. Eckstein, *Phys. Rev. B* **64**, 132406 (2001).
- ³⁰B. Raquet, A. Anane, S. Wirth, P. Xiong, and S. von Molnár, *Phys. Rev. Lett.* **84**, 4485 (2000).
- ³¹R. D. Merithew, M. B. Weissman, F. M. Hess, P. Spradling, E. R. Nowak, J. O'Donnell, J. N. Eckstein, Y. Tokura, and Y. Tomioka, *Phys. Rev. Lett.* **84**, 3442 (2000).
- ³²F. M. Hess, R. D. Merithew, M. B. Weissman, Y. Tokura, and Y. Tomioka, *Phys. Rev. B* **63**, 180408 (2001).
- ³³R. Mathieu, P. Svedlindh, R. Gunnarson, and Z. G. Ivanov, *Phys. Rev. B* **63**, 132407 (2001).
- ³⁴L. I. Glazman and K. A. Matveev, *Zh. Éksp. Teor. Fiz.* **94**, 332 (1988) [*Sov. Phys. JETP* **67**, 1276 (1988)].
- ³⁵R. Gross, in *Interfaces in Superconducting Systems*, edited by S. L. Shinde and D. Rudman (Springer, New York, 1994), pp. 176–209.
- ³⁶R. Gross, L. Alff, A. Beck, O. M. Froehlich, D. Koelle, and A. Marx, *IEEE Trans. Appl. Supercond.* **7**, 2929 (1997).
- ³⁷M. F. Chisholm and S. J. Pennycook, *Nature (London)* **351**, 47 (1991).
- ³⁸B. Kabius, J. W. Seo, T. Amrein, U. Dahne, A. Scholen, M. Siegel, K. Urban, and L. Schultz, *Physica C* **231**, 123 (1994).
- ³⁹J. W. Seo, B. Kabius, U. Dahne, A. Scholen, and K. Urban, *Physica C* **245**, 25 (1995).
- ⁴⁰J. Mannhart, *Supercond. Sci. Technol.* **9**, 49 (1996).
- ⁴¹J. Mannhart and H. Hilgenkamp, *Mater. Sci. Eng., B* **56**, 77 (1998).
- ⁴²A. Marx and R. Gross, *Appl. Phys. Lett.* **70**, 120 (1997).
- ⁴³M. Jullière, *Phys. Lett. A* **54**, 225 (1975).
- ⁴⁴G. G. Cabrera and N. Garcia, *Appl. Phys. Lett.* **80**, 1782 (2002).
- ⁴⁵M. Ziese, C. Srinithiwarawong, and C. Shearwood, *J. Phys.: Condens. Matter* **10**, L569 (1998).
- ⁴⁶S. Ingvarsson, G. Xiao, R. A. Wanner, P. Trouilloud, Y. Lu, W. J. Gallagher, A. Marley, K. P. Roche, and S. S. Parkin, *Appl. Phys. Lett.* **85**, 5270 (1999).
- ⁴⁷S. Ingvarsson, G. Xiao, S. S. Parkin, W. J. Gallagher, G. Grinstein, and R. H. Koch, *Phys. Rev. Lett.* **85**, 3289 (2000).
- ⁴⁸N. Furukawa, *J. Phys. Soc. Jpn.* **66**, 2523 (1997).
- ⁴⁹R. Jansen and J. S. Moodera, *Phys. Rev. B* **61**, 9047 (2000).